



INSTITUTE OF THEORETICAL
AND EXPERIMENTAL PHYSICS

V.E. Markushin

LIGHT EXOTIC ATOMS
IN LIQUID AND GASEOUS HYDROGEN AND DEUTERIUM.
ATOM $\bar{p}p$, THEORY AND EXPERIMENT

M O S C O W 1 9 8 0

A b s t r a c t

We consider the de-excitation, absorption and Stark mixing processes in light exotic atoms formed in liquid and gaseous hydrogen (deuterium) and present the new method of the cascade calculations. Atom $\bar{p}p$ is studied in detail, calculated are: the populations of atomic levels, the absorption probabilities, and the X-rays yields. We discuss the present-day experimental data and conclude that all of them (but one result), can be easily reconciled with each other and with the theory.

I. INTRODUCTION

Protonium - $\bar{p}p$ atom - seems to become of the utmost interest among the hadronic atoms in the nearest future. The point is that besides Coulomb levels there exist bound and resonant states in $\bar{p}p$ system (baryonium) which manifest themselves in variety of effects when \bar{p} and p form $\bar{p}p$ atom /1-3/. It is worth to mention gamma transitions from the atomic to the quasinuclear states /4,5/, the positive nuclear shift of the atomic 1S level (due to the below-threshold baryonium level with $l=0$ /6,7/), abnormally large P-wave annihilation at rest /8-10/.

Several experiments with $\bar{p}p$ atoms /5,9-12/ turned out to be rather informative (as we will see below), however, we have not yet firmly established the picture of the processes in $\bar{p}p$ atom, hence further investigations in this field are necessary. To a large extent this program will be boosted by the Low energy antiproton ring (LEAR) at CERN. Of great interest is $\bar{p}d$ atom as well, in particular, quasi-nuclei $2\bar{N}\bar{N}$ formation is possible in this case.

Besides $\bar{p}p$ and $\bar{p}d$, other light exotic atoms, e.g., $\bar{K}p$ and $\bar{\mu}d$, attract attention. Recent experiments with $\bar{K}p$ atom found unexpectedly small nuclear shift of 1S level /13/, and this fact enforces us to reconsider our knowledge about K - N interaction. Problems connected with $\bar{\mu}d$ atom arise when studying μ catalysis of the reaction $d + t \rightarrow {}^4\text{He} + n$ /14/.

The atoms mentioned above are the simplest, consisting of two oppositely charged particles. In contrast to the

heavy exotic atoms with nuclear charge $Z > 1$, they have no electrons of their own and, being rather small and neutral, pass freely through the electron clouds of neighbouring atoms. The strong in-atomic electric field causes the intensive transitions among the sublevels of given principal quantum number n , the importance of this effect has been established by Day, Snow and Sucher ^{/15/}. Thus, besides de-excitation and absorption, there is Stark mixing which makes the atomic cascade very complicated and sensitive to the environment.

In this paper we deal with the problem of the cascade calculations in the light exotic atoms. Our main aim is the theoretical study of the cascade processes in $\bar{p}p$ atom in liquid and gaseous hydrogen. The first estimates of the rates of antiproton absorption from atomic states have been done by Desai in 1960 ^{/16/}. Later Delkarov et al. ^{/2,3/} performed the detailed cascade calculations for $\bar{p}p$ and $\bar{p}d$ atoms in liquid hydrogen and deuterium using the effective rates method developed and applied to the $\bar{\alpha}p$ and $\bar{K}p$ mesonic atoms by Leon and Bethe ^{/17,18/}. The antiprotonic atom in gaseous hydrogen and deuterium has been theoretically studied by the author in ^{/19/} with the more general method of the cascade calculations. The central problem considered in Ref. ^{/2,3,19,20/} was how the existence and properties of $\bar{N}N$ quasinuclear states influence the properties of $\bar{p}p$ atom. Because of the lack of necessary experimental information, several hypotheses about the quantitative properties of quasinuclei $\bar{N}N$ spectra were assumed and predicted were the specific properties of the atomic cascades. It is worth mentioning that these investigations had been done before $\bar{p}p$ atom has been observed experimen-

tally ¹¹¹, and hence the predictions were mainly qualitative. The experiments carried out in recent time enable us to avoid many uncertainties involved in previous theoretical papers and to obtain not only qualitative description of $\bar{p}p$ atoms cascade process, but a set of quantitative predictions as well.

The plan of the paper is the following. The first part is entirely methodic. Section 2 contains preliminary information. Section 3 is devoted to the method of the cascade calculation which enables one to calculate populations of atomic levels, absorption probabilities and intensities of transitions between different levels. The second part of the paper is devoted to $\bar{p}p$ atom. The main experimental data are compiled in Sec.4. The theoretical analysis of the cascade processes and results of the cascade calculations are given in Sec.5. The relevance of the theory to the experiment is discussed in Sec.6. The concluding remarks are given in Sec.7.

2. PRELIMINARY INFORMATION

In this section we have compiled some facts about the de-excitation, the Stark mixing and the nuclear shifts and widths of atomic levels. They concern those aspects of the relationship between the different cascade processes, which are the most essential for the development of the method of the cascade calculations, and show the characteristic scales of the values involved. The details can be found in the original papers cited below. As for $\bar{p}p$ atom, the detailed description including the calculated values of the de-excitation, absorption and Stark mixing rates

and the experimental data will be given in Sect.5, 6.
 For definiteness, we speak of protonium, the same is valid
 for other light exotic atoms with nuclear charge $Z = 1$,
 unless indicated otherwise. The units used are: $\hbar = c = 1$,
 $e^2 = \alpha = 1/137$.

The ground state Coulomb binding energy \mathcal{E}_{1S} and Bohr
 radius a_1 for the hydrogen like atom of reduced mass
 M are given by the formulas

$$\mathcal{E}_{1S} = M\alpha^2/2$$

$$a_1 = (\alpha M)^{-1}$$

For $\bar{p}p$ atom

$$M = m_p/2 \quad \mathcal{E}_{1S} = 12.5 \text{ KeV}$$

$$a_1 = 57.6 \text{ fm}$$

De-excitation processes

To be captured into atomic orbit the antiproton moving
 in hydrogen has to slow down to the energy about
 several tens KeV ^{/21,22/}. Having been formed in high
 excited states n with Bohr radius a_n comparable with
 that of hydrogen atom $a_H = (\alpha m_e)^{-1}$, i.e. $n \approx (m_p/2m_e)^{1/2} \approx$
 ≈ 30 , the protonium cascades down by means of chemical
 process $\bar{p}p + H_2 \rightarrow \bar{p}p + H + H$, external Auger effect
 $\bar{p}p + H_2 \rightarrow \bar{p}p + H_2^+ + e^-$, and radiation $\bar{p}p \rightarrow \bar{p}p + \gamma$
 (see for details ^{/17/}). The initial stage where the most
 important role belongs to the chemical de-excitation is
 badly explored. The protonium is expected to have got
 about 1 eV kinetic energy (velocity $v \sim 10^6$ cm/sec) as
 a result of H_2 dissociation. Auger transitions are mainly
 of the dipole type ($\Delta l = l_i - l_f = \pm 1$), transitions

with minimal change in n , consistent with H_2 ionisation energy, being favourable. The rate of Auger de-excitation $\Gamma_{n\ell n\ell}^e$ was calculated in Born approximation in Ref. ^{17/}. The Auger de-excitation dominates over the chemical one at

$n \lesssim 15$. For the largest few n ($n = 10-12$), for which $\Delta n = 1$ is possible, the Auger de-excitation rate is rather fast: $\Gamma_n^e > N V \Omega C_H^2$ (N is the hydrogen density, for the hydrogen bubble chamber $N V \Omega C_H^2 = 3.5 \cdot 10^{12} \text{ sec}^{-1}$). As n decreases, Auger rate drops off rapidly, so that the radiative de-excitation becomes important at the final stage of the cascade. The radiative de-excitation rate $\Gamma_{n\ell n\ell}^x$ is given by the well-known formula

$$\Gamma_{i\ell}^x = \frac{4}{3} \alpha R_{i\ell}^2 \omega_{i\ell}^3$$

The typical values for protonium are

$$\Gamma_{2p,1s}^x = 3.8 \cdot 10^{-4} \text{ eV}$$

$$\Gamma_{3s,2p}^x = 3.9 \cdot 10^{-5} \text{ eV}$$

In liquid hydrogen (density $N_0 = 4.26 \cdot 10^{22} \text{ cm}^{-3}$) the radiation prevail over the Auger effect at $n_f < 3$. In gaseous hydrogen with the density $N = 5 \cdot 10^{-3} N_0$ (pressure 4 atm at $T = 300^\circ\text{K}$) the radiation dominates the excitation at $n_f < 6$.

Para- and ortho-protonium

Due to the CP invariance of the electromagnetic and strong interactions the states of protonium can be characterized by such an exact quantum number as spin $S = 0, 1$. It follows from the fact that the CP-parity of the system consisting of the fermion-antifermion pair and the spin S are uniquely related

$$CP = (-1)^{1+S}$$

Thus, there are two kinds of $\bar{p}p$ atoms - paraprotonium ($S = 0$) and ortoprotonium ($S = 1$), the spin S being conserved in the cascade.

Nuclear shift and width of atomic level

The strong interaction causes an energy shift ΔE and broadening Γ of the atomic level. The S- and P-state energy displacement $\Delta E - i\frac{\Gamma}{2}$ can be expressed in terms of the S- wave scattering length A_S and P- wave scattering volume (A_P/κ^2) by the well-known formulas^[23]

$$\Delta E_{nS} - i\frac{\Gamma_{nS}}{2} = -\frac{2\pi}{M} |\psi_{nS}(0)|^2 A_S \quad (1)$$

$$\Delta E_{nP} - i\frac{\Gamma_{nP}}{2} = -\frac{6\pi}{M} |\nabla\psi_{nP}(0)|^2 \frac{A_P}{\kappa^2}$$

For protonium

$$\Delta E_{nS} - i\frac{\Gamma_{nS}}{2} = \frac{0.867}{n^3} \text{ keV} \cdot \text{fm}^{-1} \cdot A_S$$

$$\Delta E_{nP} - i\frac{\Gamma_{nP}}{2} = \frac{32(n^2-1)}{3n^5} \cdot 2.45 \cdot 10^{-2} \text{ eV} \cdot \text{fm}^{-3} \cdot \frac{A_P}{\kappa^2}$$

Formulas (1) are valid provided the scattering lengths are small in comparison with the Bohr radius $a_1 = 57.6 \text{ fm}$, otherwise the more careful treatment is needed^[17].

The present day data on NN scattering do not allow one to establish with confidence A_S and A_P/κ^2 . The experimental data on ΔE and Γ will be considered in Sect.5 As for the theoretical predictions, they are model dependent:

$$\begin{aligned} \Delta E_{1^1S_0} &= 0.7 \text{ keV} & \Gamma_{1^1S_0} &= 1.7 \text{ keV} \\ \Delta E_{1^3S_1} &= 0.8 \text{ keV} & \Gamma_{1^3S_1} &= 1.3 \text{ keV} \end{aligned} \quad [24]$$

$$\begin{aligned} \Delta E_{1^1S_0} &= 0.5 \text{ keV} & \Gamma_{1^1S_0} &= 0.3 \text{ keV} \\ \Delta E_{1^3S_1} &= 0.6 \text{ keV} & \Gamma_{1^3S_1} &= 0.3 \text{ keV} \end{aligned} \quad [25]$$

One can expect that the widths Γ_{1S} and Γ_{2P} are in the following ranges /8/

$$\begin{aligned} \Gamma_{1S} &= 50 \div 500 \text{ eV} \\ \Gamma_{2P} &= 5 \cdot 10^{-4} \div 10^{-2} \text{ eV} \end{aligned}$$

For the protonium states $n\ell$ with $\ell > 1$ the annihilation widths are much smaller than the radiative de-excitation widths.

Stark mixing

The $\bar{p}p$ atom, when moving in matter, drifts through the electric field of hydrogen atoms. It is easy to understand that resulting Stark mixing plays a significant role for $\bar{p}p$ atom in liquid hydrogen. The frequency of the Stark transitions $n\ell \leftrightarrow n(\ell-1)$ in the electric field $\mathcal{E} = \alpha^{1/2} \cdot \Omega_H^2$ is given by the formula

$$\omega_{St} = \langle n\ell | \alpha^{1/2} \vec{r} \vec{\mathcal{E}} | n(\ell-1) \rangle = \alpha \Omega_H^2 \langle n\ell | r | n(\ell-1) \rangle = n(n^2 - \ell^2)^{1/2} \cdot 4 \cdot 10^{13} \text{ sec}^{-1}$$

The characteristic time of the Stark mixing (the time of flight through the interior of the hydrogen atom) is

$$\tau_{St} = \Omega_H / \nu = 0.5 \cdot 10^{-14} \text{ sec}^{-1}$$

Therefore $\omega_{St} \cdot \tau_{St} \gg 1$, what means that the $\bar{p}p$ atom, when passing through the hydrogen atom, makes many transitions back and forth among the states of given n . The rate of the Stark collisions should be of the scale $Nv\sigma_{St}^2$ ($3.5 \cdot 10^{-12} \text{ sec}^{-1}$ for liquid hydrogen), so the Stark mixing significantly affects the de-excitation and absorption unless the liquid hydrogen is replaced by the gaseous one. We shall see below that at the hydrogen density $N = 10^{-3} N_0$ the Stark mixing becomes negligible in states $n < 5$. The most important consequences of the Stark mixing the intensive absorption at high n via the S state mixed with the states $\ell > 0$ (the Day-Snow-Sucher mechanism) /15/.

To calculate the Stark mixing effects, Leon and Bethe have developed the impact parameter method /17/. Treating the atom as moving along definite and undeflected trajectory through the electric field of hydrogen atom they have found the $n\ell \rightarrow n'\ell'$ transition probability as a function of impact parameter g and velocity v

$$T_{n\ell \rightarrow n'\ell'} = T(n, \ell, n', \ell', g, v)$$

The results can be summarized as following (see /17,26,2/)

1. Significant are only the transitions between the states of the same n .
2. There exists the critical value of the impact parameter g_n beyond which ($g > g_n$) the probability of any Stark transition is negligibly small. Thus, one can easily define the notion of the Stark collision rate

$$\Gamma_n^{St} = Nv\sigma g_n^2 \quad (2)$$

and the probability of the transition $n\ell \rightarrow n\ell'$ in the Stark collision

$$T_n(\ell, \ell') = g_n^{-2} \int_0^{g_n^2} dg^2 T(n, \ell, \ell', g, v)$$

3. After the Stark collision the $\bar{p}p$ atom has forgotten its own initial state because the intensity of the Stark mixing is very large at $g < g_n$ ($\omega_{st} \cdot \tau_{st} \gg 1$). It means that $T_n(\ell, \ell')$ is independent on ℓ and determined by the statistical weight of the final state ℓ'

$$T_n(\ell, \ell') = (2\ell'+1)/n^2$$

The statement (3) is valid for n^2 degenerate states. For protonium the nuclear shift of the nS level with respect to the levels $n\ell$ ($\ell > 0$) is not small in comparison with the Stark splitting. In fact, the Stark splitting of the states of given n in the electric field $\mathcal{E} = \alpha^{1/2} \alpha_H^{-2}$ (the linear Stark effect) is

$$\Delta E_n^{st} = 3\alpha n(n-1)\alpha_H / \alpha_H^2 \sim 0.1 \text{ eV} \cdot n^2$$

while the nuclear displacement of the nS level

$$|\Delta E_{nS} - i\Gamma_{nS}/2| \sim 1 \text{ keV} \cdot n^{-3}$$

therefore $|\Delta E_{nS} - i\Gamma_{nS}/2| \gg \Delta E_n^{st}$ at $n \leq 8$.

Thus, the essential Stark mixing between the S -state and the states $\ell > 0$ is possible only for those values of impact parameter g which allow the $\bar{p}p$ atom to pass through the region where the electric field is strong enough for the Stark splitting to overcome the energy displacement of the S -state. It means that, when $\bar{p}p$ atom

moves in hydrogen, the strongly shifted S- state is mixed with the other states considerably slower than they are mixed with each other, and the greater the nuclear shift ΔE_{1S} were, the smaller would be the rate of the S- state absorption via the Stark mixing. The problem of the Stark mixing in the presence of the nuclear interaction has been treated in ^{/17/}. The results of calculations for protonium will be considered in Sect.6 (see also ^{/2,3/}).

3. METHOD OF CASCADE CALCULATIONS

In this section we describe the general method of the cascade calculations for the light exotic atoms in liquid and gaseous hydrogen (deuterium). To introduce the notions of the occupation probabilities and the conditional probabilities of the transitions and absorption we concern briefly the cascade calculations for an isolated atom. Then we specify the Stark mixing model and introduce the notions of incoming and outgoing probabilities. We find it useful and suggestive to sketch the atomic cascade as a flow graph and describe it as Markov chain. The problem of the cascade calculations is solved by the standard methods of the Markov chains theory. Finally, the method of the effective rates ^{/17/} is concerned as the extremal case of our method at the large Stark mixing rates.

An isolated atom

If there is no Stark mixing between atomic states, it is quite easy, given an initial population and transition and absorption rates, to calculate the transition and absorption probabilities. Let, for the state $n\ell$, $P_{n\ell}$

be its occupation probability, $\Gamma_{n\ell n'\ell'}$ - the rate of the transition to the state $n'\ell'$, and $\Gamma_{n\ell}^a$ - the rate of the absorption. Then the conditional probabilities^{*)} of the transition $t_{n\ell n'\ell'}$ and the absorption $C_{n\ell}$ are defined by the formulas

$$t_{n\ell n'\ell'} = \Gamma_{n\ell n'\ell'} / \Gamma_{n\ell}^{\text{tot}} \quad (3)$$

$$C_{n\ell} = \Gamma_{n\ell}^a / \Gamma_{n\ell}^{\text{tot}} \quad (4)$$

where

$$\Gamma_{n\ell}^{\text{tot}} = \sum_{n'\ell'} \Gamma_{n\ell n'\ell'} + \Gamma_{n\ell}^a \quad (5)$$

Consider the finite number of states having been populated, with the initial population being of the form

$$P_{n\ell} = 0, \quad n > N \quad (6)$$

$$P_{n\ell} = P_{n\ell}^{(N)}, \quad n \leq N$$

Then the probabilities of the transitions between the states $n\ell$ and $n'\ell'$ with $n=N$ are determined immediately

$$y_{N\ell n'\ell'} = P_{N\ell}^{(N)} \cdot t_{N\ell n'\ell'} \quad (7)$$

and so does the probability of the absorption in the state $N\ell$

$$\Gamma_{N\ell} = P_{N\ell}^{(N)} \cdot C_{N\ell} \quad (8)$$

The transitions $N\ell \rightarrow n'\ell'$ cause the occupation probabilities to change as following

*) The conditional probability of a process is equal to the absolute probability of this process provided the initial state is populated with the unit probability.

$$P_{n\ell}^{(N)} \rightarrow P_{n\ell}^{(N-1)} = 0$$

$$P_{n\ell}^{(N)} \rightarrow P_{n\ell}^{(N-1)} = P_{n\ell}^{(N)} + \sum_{\ell'} y_{n\ell'\ell} , \quad n < N \quad (9)$$

Thus, we get the initial population of the form (6) with $N \rightarrow (N - 1)$ and can continue the calculations by iterating the operations (7) + (9). The characteristic feature of this procedure is that the cascade processes are treated in the order of the level sequence but not as they develop in time.

Atom in matter

When the atom moves in matter, the Stark mixing is significant only for the states of the same principal quantum number n , therefore we can consider the cascade processes as evolved in the order of decreasing n . Consider the atom on the way between the subsequent Stark collisions, the mean time of flight is $\tau = 1/\Gamma_n^{\text{st}}$ where Γ_n^{st} is the rate of the Stark collisions (2). The atom either does not change its initial state $n\ell$ during this interval with probability

$$S_{n\ell} = \exp(-\Gamma_{n\ell}^{\text{tot}}/\Gamma_n^{\text{st}}) \quad (10)$$

or leaves it by de-excitation or absorption with probability

$$g_{n\ell} = 1 - S_{n\ell} \quad (11)$$

After the Stark collision the atom has forgotten its initial state, hence the state $n\ell$ is occupied with the

conditional probability *)

$$q_{n\ell} = (2\ell+1)/n^2 \quad (12)$$

The relationship between the different cascade processes becomes visual if we sketch the cascade by the flow graph, nodes of which represent atomic states and edges correspond to transitions among them. The edges are characterized by the conditional transition probabilities, the states of nodes - by the occupation probabilities. There are following nodes in our case:

1. The nodes $n\ell$ corresponding to the atomic states $n\ell$ between the Stark collisions.
2. The nodes Z_n that correspond to the atomic states during the Stark collision.
3. The nodes $\tilde{n}\ell$ that denote the sets of states, for which the atom leaves the state $n\ell$ during the time between the Stark collisions. Their occupation probabilities $\tilde{p}_{n\ell}$ are defined as the sum of the probabilities of the transitions from the state $n\ell$ to the states $n'\ell'$ with $n' < n$ and the absorption probability in the state $n\ell$.
4. The nodes $A_{n\ell}$ represent the absorption in the state $n\ell$.

*) The case when the S- state energy displacement and the absorption during the Stark collision are significant will be considered below.

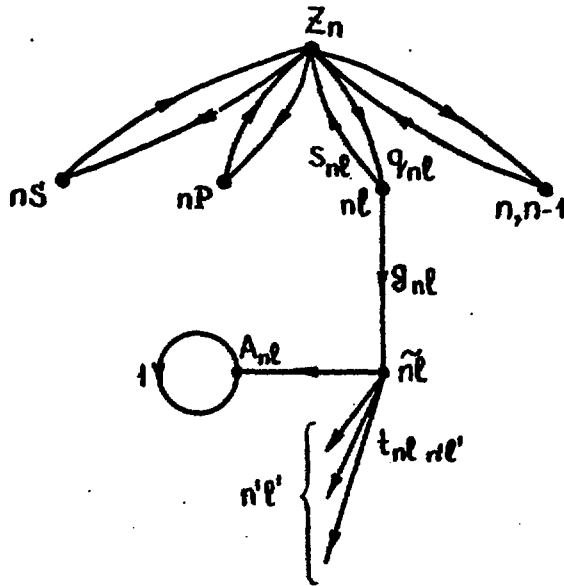


Fig. 1

The graph is plotted in Fig.1. The conditional transition probabilities satisfy the normalization conditions: the sum of the conditional transition probabilities over all the transitions from the given state is equal to unity. The graph thus defined can be interpreted as a finite Markov chain that allows us to manage with it using the standard methods of the Markov processes theory [27].

Assume the initial population to have the form

$$\begin{aligned}
 P_{nl} &= 0, \quad n > N \\
 P_{nl} &= P_{nl}^{(n)}, \quad n \leq N
 \end{aligned}
 \tag{13}$$

We shall refer to the occupation probabilities $P_{nl}^{(n)}$ with $n=N$ as the total incoming populations of the state nl . The probabilities of the absorption in and the transitions from the states nl are calculated as follows.

Consider the subgraph consisting of the nodes with $n=N$ and the corresponding edges (see Fig.2). For the sake

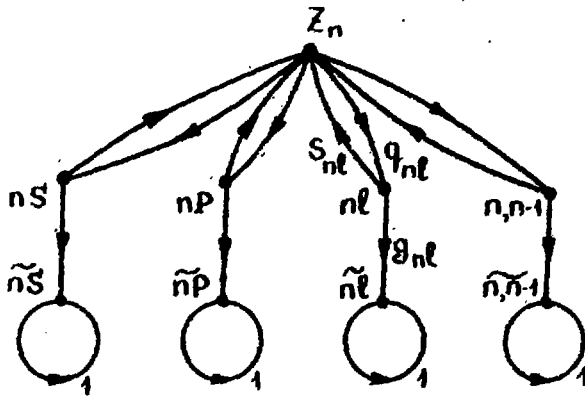


Fig. 2

of convenience we redenote the nodes as P_i , $i=1, 2n+1$. The nodes of the subset $\{P_i, i=1, n\} = \{\tilde{P}_{nl}, l=0, n-1\}$ will be referred to as absorbing states because no transitions from them to the other states are possible in the subgraph concerned. The rest of the states $\{P_i, i=n+1, 2n+1\} = \{P_{nl}, l=0, n-1; Z_n\}$ will be referred to as the transient ones. The conditional probabilities of the transitions $P_i \rightarrow P_j$ form the transition matrix \mathbb{P}

$$\mathbb{P} = (P_{ji}) = \begin{pmatrix} \mathbf{I} & \mathbf{G} \\ \mathbf{0} & \mathbf{Q} \end{pmatrix} \quad (14)$$

Here \mathbf{G} is the matrix $n \times (n+1)$ which describes the transitions from the transient states $\{P_i, i=n+1, 2n+1\}$ to the absorbing states $\{P_i, i=1, n\}$

$$G = \begin{pmatrix} g_{ns} & & & 0 \\ & g_{np} & & \\ & & g_{nl} & \\ 0 & & & g_{nn-1} \end{pmatrix} \quad (15)$$

Q is the matrix $(n+1) \times (n+1)$ corresponding to the transitions among the transient states

$$Q = \begin{pmatrix} & & & q_{ns} \\ & 0 & & q_{nl} \\ & & & q_{nn-1} \\ \hline s_{ns} & s_{np} & s_{nn-1} & 0 \end{pmatrix} \quad (16)$$

I is the unit matrix $n \times n$ and O is the zero matrix $(n+1) \times n$. The representation of the transition matrix P in the form (14) explicitly indicates that the states $\{\rho_i, i=1, n\}$ are the absorbing ones (see Fig2).

Consider the matrix $B = (B_{ij})$, the elements of which B_{ij} , by definition, are the probabilities the process starting in the transient state ρ_{nj} to terminate in the absorbing state ρ_i . This matrix satisfies the equation /27/

$$B = G + B \cdot Q \quad (17)$$

the solution of which has the form

$$B = G \cdot N \quad (18)$$

where $N = (I - Q)^{-1}$ is the fundamental matrix.

With the matrix B having been calculated and the incoming occupation probabilities P_{nl} given, we can determine the resulting occupation probabilities \tilde{P}_{nl} (the nodes Z_n and \tilde{P}_{nl} are assumed to be of zero occupation probability at the initial moment):

$$P_{\kappa} = \sum_{i=1}^n B_{\kappa i} P_i, \quad \kappa \equiv \tilde{n}l, \quad i \equiv nl. \quad (19)$$

We shall call \tilde{P}_{nl} as the outgoing occupation probabilities of the states nl , they play the same role as P_{nl} do in the absence of the Stark mixing. The probabilities of the transitions from the states nl and the probabilities of the absorption in the states nl are given by the formulas

$$Y_{nl \ n'l'} = \tilde{P}_{nl} \cdot t_{nl \ n'l'} \quad (20)$$

$$\Gamma_{nl} = \tilde{P}_{nl} \cdot C_{nl} \quad (21)$$

where $t_{nl \ n'l'}$ and C_{nl} were defined earlier (3), (4).

As the result of the processes concerned the occupation probabilities P_{nl} change in the following way

$$\begin{aligned} P_{nl}^{(N)} \rightarrow P_{nl}^{(N-1)} &= 0 \\ P_{nl}^{(N)} \rightarrow P_{nl}^{(N-1)} &= P_{nl}^{(N)} + \sum_{l'} Y_{Nl' \ nl} \end{aligned} \quad (22)$$

Thus, we can calculate step by step ($N \rightarrow N-1$) the outgoing occupation probabilities and the probabilities of the transitions and absorptions in the presence of the Stark mixing.

For the sake of simplicity we disregard the problem concerned with the influence of the S- state energy displacement with respect to the states with $l > 0$ on the Stark mixing and that of the absorption during the Stark collision. The first has already been mentioned in Sec.2. As for the second, it is also of great importance, in which we convince ourselves by comparing the annihilation widths of the protonium S' states $\Gamma_{nS}^a \sim 10^2 \text{ eV/n}^3$ to the characte-

istic time of the Stark collision $\tau_{st} \sim Q_H / v \approx 8eV^{-1}$;
 $\tau_{st} \Gamma_{n3}^q \gg 1$ for $n \leq 8$. These problems introduce considerable complications and have not yet been completely solved. The suggestive estimations of the absorption rate have been done by Leon and Bethe in the "fixed field model" /18/.

Using the results obtained in /17,26/ we have constructed the model of the cascade processes in $\bar{p}p$ and $\bar{p}d$ atoms in liquid and gaseous hydrogen and deuterium /19/. Here we give only the sketch of the graph (see Fig.3).

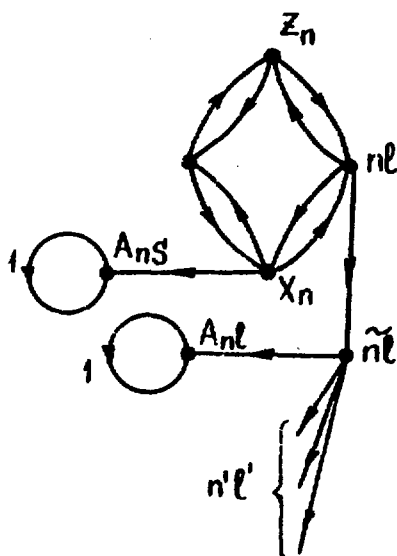


Fig. 3

The definitions of the transition probabilities, being of rather bulky form, can be found in /19/. The atomic states during the Stark collisions are described by two nodes,

Z_n and X_n . The node X_n stands for the subset of states which can be mixed with the S state^{*)}.

^{*)}In the fixed field model /17/ the node X_n corresponds to the states with magnetic quantum number $m = 0$, the quantization axis being taken along the direction of the electric field.

The probability of the transitions between the nodes X_n and nS tends to zero as the S- state energy displacement increases. The node \sum_n corresponds to the subset of states, the coupling of which to the S- state by the Stark mixing is negligible. The edge $X_n \rightarrow A_{nS}$ describes the S state absorption during the Stark collision.

The method of the effective rates

If the Stark mixing rate is much bigger than the de-excitation and absorption rates then the sublevels $n\ell$ of given n are populated in accordance with their statistical weight $(2\ell+1)/n^2$. Thus, to be determined are only the total occupation probabilities $P_n = \sum_{\ell} P_{n\ell}$. This can be done by means of the effective rates method^{/17/}. The de-excitation is characterized by the effective de-excitation rate

$$\Gamma_{nn'} = \Gamma_n^{st} \sum_{\ell, \ell'} \frac{(2\ell+1)}{n^2} \left(1 - \exp\left(-\frac{\Gamma_{n\ell}^{tot}}{\Gamma_n^{st}}\right)\right) \frac{\Gamma_{n\ell n'\ell'}}{\Gamma_{n\ell}^{tot}} \approx \quad (23)$$

$$\left(\frac{\Gamma_n^{st}}{\Gamma_n^{tot}}\right) \rightarrow \infty \quad \sum_{\ell, \ell'} \frac{(2\ell+1)}{n^2} \Gamma_{n\ell n'\ell'}$$

The P state absorption is characterized by the effective rate

$$\Gamma_n^{P-abs} = \frac{3}{n^2} \Gamma_n^{st} \left(1 - \exp\left(-\frac{\Gamma_{nP}^{tot}}{\Gamma_n^{st}}\right)\right) \frac{\Gamma_{nP}^a}{\Gamma_{nP}^{tot}} \quad (24)$$

As for the S state absorption, its effective rate Γ_n^{S-abs} does not have such an obvious definition as the above described ones do, and we omit it here. The details can be found in^{/17,2,3/}, and the results of the numerical calcu-

lations for protonium will be given in Sect.5.

With the effective rates thus defined, the conditional probabilities of the S- and P- state absorption Γ_n^S and Γ_n^P and the conditional probability of the transitions between the states n and n' $t_{nn'}$ are determined by formulas

$$\Gamma_n^{(S,P)} = \Gamma_n^{(S,P)\text{-abs}} / \Gamma_n^{\text{tot}} \quad (25)$$

$$t_{nn'} = \Gamma_{nn'} / \Gamma_n^{\text{tot}} \quad (26)$$

where

$$\Gamma_n^{\text{tot}} = \sum_{n'} \Gamma_{nn'} + \Gamma_n^{\text{S-abs}} + \Gamma_n^{\text{P-abs}} \quad (27)$$

One can show that the above described general method of the cascade calculations at $\Gamma_n^{\text{st}} / \Gamma_n^{\text{tot}} \gg 1$ gives rise to that of effective rates, with the graph on Fig.1 and the conditional probabilities involved serving as an obvious suggestion for the definitions of the effective rates.

PROTONIUM - EXPERIMENT AND THEORY

4. EXPERIMENTAL DATA

The present day experimental data on the low-energy $\bar{N}N$ interaction and the protonium properties are far from completeness, they all should be considered as suggestive rather than firmly established because of their coming from the unique experiments. Here we remind some of them very briefly.

The P- wave contribution into orthoprotonium annihilation

Due to the total angular momentum and parity conservation, the processes $\bar{p}p \rightarrow 2\pi, 2K$ are possible only from the triplet states $\bar{p}p$ ($S=1$), only the odd orbital angular momenta l contributing to the annihilation into two identical mesons ($2\pi^0, 2K_S$) /9,10,28/. Hence, studying the $\bar{p}p$ annihilation in 2π and $2K$ "at rest" which practically takes place from the atomic states /2/ one can judge upon the P- wave contribution into the orthoprotonium annihilation. The data on the annihilation $\bar{p}p \rightarrow \pi^+\pi^-, 2\pi^0$ suggest the large P- wave contribution

$$R_S = \frac{\bar{p}p \rightarrow 2\pi |l\text{-odd}}{\bar{p}p \rightarrow 2\pi |l\text{-all}} \approx \frac{\bar{p}p \rightarrow 2\pi |l=1}{\bar{p}p \rightarrow 2\pi |l=0,1}$$

$$\begin{aligned} R_S &= 0.39 \pm 0.08 \quad /9/ \\ R_S &= 0.13 \pm 0.04 \quad /10/ \end{aligned} \quad (28)$$

while the data on the processes $\bar{p}p \rightarrow K_L K_S, 2K_S$ support the hypothesis that the S- wave dominates the absorption

$$R_K = 0.015 \begin{matrix} +0.012 /28/ \\ -0.005 \end{matrix} \quad (29)$$

The process $\bar{p}p \rightarrow 2K_s$ is probably suppressed due to the dynamical reason as it has been pointed out in ^{/8/}.

The gamma transitions
between protonium and baryonium states

The evidence for the γ - transitions between the atomic $\bar{p}p$ levels and the quasinuclear $N\bar{N}$ levels has been found in the experiment of Karlsruhe-Basel-CERN-Stockholm-Strasbourg collaboration (see Table 1) ^{/5/}.

Table 1
 γ - transitions from atomic to quasinuclear states ^{/5/}

Energy (MeV)	Apparatus Width (MeV)	Confidence Level (%)	Intensity
183 ± 7	19	99,0	$(7,2 \pm 1,7) \cdot 10^{-3}$
216 ± 9	21	97,5	$(6,0 \pm 1,9) \cdot 10^{-3}$
420 ± 17	34	98,2	$(8,5 \pm 2,0) \cdot 10^{-3}$

The transitions of this kind were predicted theoretically before their experimental search ^{/4/}. The most intensive are the E1 transitions from the S- states of $\bar{p}p$ atom to the P- states of the quasinuclear baryonium, for the transitions with energy $\omega = 200 - 500$ MeV the 1S state radiative width should be about $\Gamma_{1S}^{\gamma} \sim 1$ eV ^{/4,29/}. The γ - rays yield is given by the formula ^{*)}

$$Y_i = \frac{\Gamma_{1S}^{\gamma_i}}{\Gamma_{1S}^{tot}} \cdot \Gamma_S \cdot K \quad (30)$$

^{*)} Both $\Gamma_{nS}^{\gamma_i}$ and Γ_{nS}^{tot} being proportional to n^{-3} , the fraction of the gamma-transition in the nS - state absorption is independent on n.

where K is the statistical weight of the initial atomic states ($K = 1/4$ and $3/4$ for para- and orthoprotonium respectively), Γ_S is the probability of the S-wave absorption.

Taking the experimental values $Y_i = (0.5-1) \cdot 10^{-2}$, $\Gamma_S = 0.6-1$ and the theoretical estimates $\Gamma_{1S}^{X_i} = 1 - 2 \text{ eV}$ we can determine the total width of the $1S$ state of "ortho-protonium with the formula (30)

$$\Gamma_{1S}^{tot} = 50 - 300 \text{ eV}$$

The X - rays of protonium

The first direct observation of the $\bar{p}p$ atom has been done by detecting the L-lines of the protonium X-rays spectrum in the experiment of CERN-Daresbury-Mainz-TRIUMF collaboration (see Table 2) ^{/11/}. The gaseous H_2 target was

Table 2

The protonium X-rays yield in the gaseous target (4 atm, 300°K, $N \approx 5 \cdot 10^{-3} \text{ No}$) ^{/7/}

Transition	Energy (KeV)	Yield
$3 \rightarrow 2$ (L_α)	1.7	$2 \cdot 10^{-2}$
$4 \rightarrow 2$ (L_β)	2.3	$1.7 \cdot 10^{-2}$
$n \geq 5 \rightarrow 2$		$2.1 \cdot 10^{-2}$
total L		$6 \cdot 10^{-2}$
$2 \rightarrow 1$ (K_α)	9.4	$\leq 6 \cdot 10^{-3}$
total K		$< 7 \cdot 10^{-2}$

used in this experiment to gain in the X-rays yield due to the suppression of the absorption via the Stark mixing and to increase the role of the radiative de-excitation.

The yield of the K_{α} - line has been estimated to be at least ten times smaller than the total L- lines yield. This means that the annihilation width of the 2P- state is sufficiently large in comparison with the width of the radiative transition $2P \rightarrow 1S$

$$\Gamma_{2P}^d \approx 10 \Gamma_{2P \rightarrow 1S}^x = 4 \cdot 10^{-3} \text{ eV}$$

The total yield of the L- lines (the population of the 2P state) and the fact of the K_{α} - line yield suppression is in agreement with those theoretical predictions which imply the strong F- state absorption /19,20/.

The observation of the K- lines of protonium has been reported in the experiment of CERN-Basel-Karlsruhe-Stockholm collaboration (see Table 3) /12/. The nuclear shift and width of the 1S state (spin = ?) were determined to be

$$\Delta E_{1S} = + 3.02 \pm 0.06 \text{ KeV}$$

$$\Gamma_{1S} \leq 0.2 \text{ KeV}$$

Table 3

Energies and intensities of $\bar{p}p$ - atom
K- lines in liquid Hydrogen /12/

Transition	Energy (KeV)	The shift	Intensity
2 - 1	6,49 \pm 0,08	2,88 \pm 0,08	2,3 $\cdot 10^{-4}$
3 - 1	8,07 \pm 0,08	3,03 \pm 0,08	2 $\cdot 10^{-4}$
4 - 1	8,36 \pm 0,18	3,35 \pm 0,18	1 $\cdot 10^{-4}$

5. THE THEORY OF THE PROTONIUM CASCADE PROCESSES

The preliminary information about the cascade processes has been given in Sect.2, now comes the time to deal with the $\bar{p}p$ atom in more detail. Firstly, we want to clarify the relationship between the different processes. To this end we have depicted in Fig.4-6 the rates of the de-excitation and Stark mixing in liquid and gaseous hydrogen.

Liquid hydrogen

It is the case when the rate of the Stark mixing is much greater than the de-excitation rates at any n (see Fig.4). Therefore, the statistical population of the sublevels of given n is maintained when the atom cascades down, and one can exploit the method of the effective rates (see Sect.3 and Ref.^{1,2,3/}). The effective rates of the de-excitation and the S- and P- state absorption are shown in Fig.7. The rate of the S- state absorption via the Stark mixing depends not only on the atomic width, but on the nuclear shift of the atomic 1S state as well, as it has been emphasized in Sect.3. To exemplify this dependence we have plotted the rates Γ_n^{S-abs} for several sets of Γ_{1s} and ΔE_{1s} . The drop of Γ_n^{S-abs} with n decreasing results from the increase of the S- state displacement $|\Delta E_{nS-i} \frac{\Gamma_{nS}}{2}|$ that prevents the S- state mixing with the states $l > 0$. Due to the same reason, the greater the energy shift ΔE_{1s} is, the smaller is the rate Γ_n^{S-abs} for the given Γ_{1s} . By comparing Γ_n^{S-abs} and the effective rate of the de-excitation $\Gamma_n = \sum_{n'} \Gamma_{nn'}$ we ascertain that the intensive S- state absorption via the Stark mixing should take

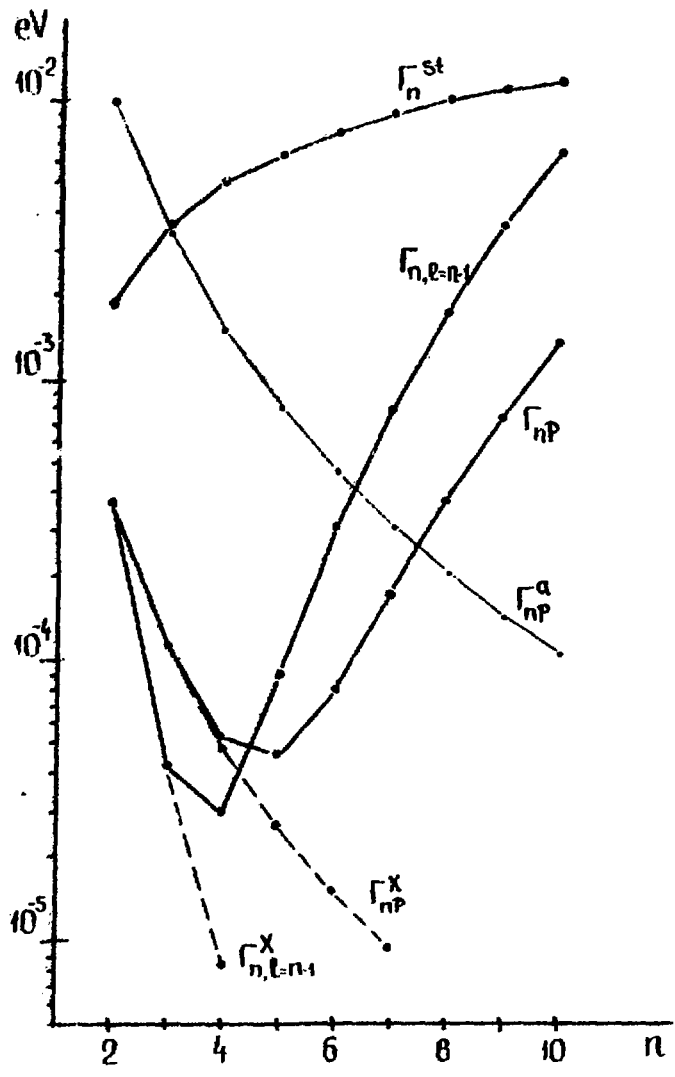


Fig. 4

The de-excitation and Stark mixing rates Γ_{nP} , $\Gamma_{n,l=n-1}$ and Γ_n^{St} in liquid hydrogen ($\bar{v} = 10^6$ cm/sec). Γ_{nP}^a is the annihilation width of the nP state, Γ_{nP}^X and $\Gamma_{n,l=n-1}^X$ are the widths of the radiative de-excitation.

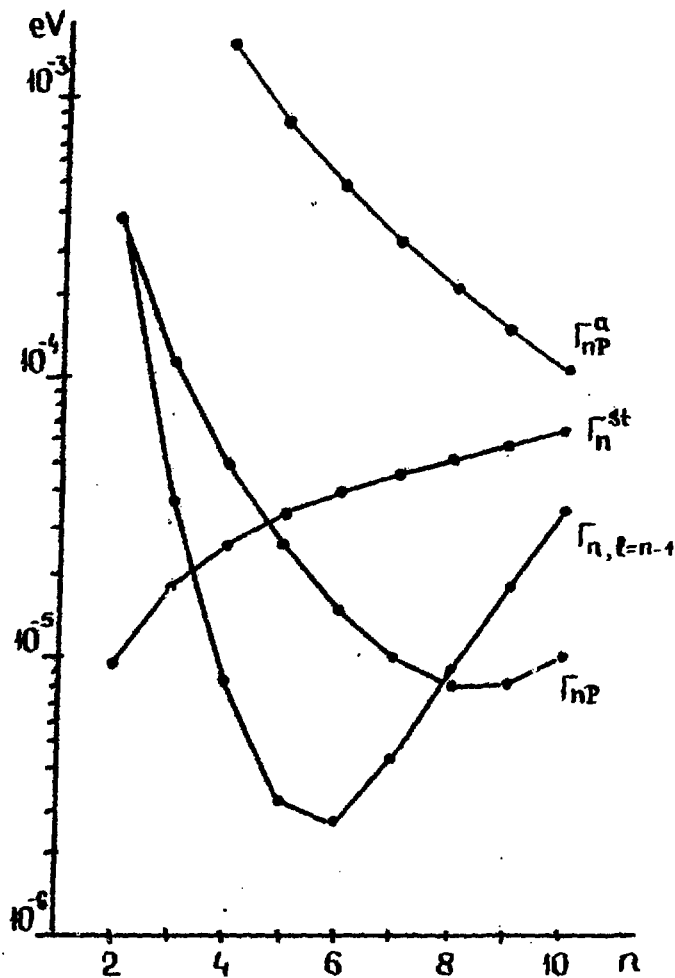


Fig. 5

The de-excitation (Γ_{nP} , $\Gamma_{n, l=n-1}$) and Stark mixing (Γ_n^{st}) rates in gaseous hydrogen ($N = 5 \cdot 10^{-3}$ No, 4atm, 300°K).

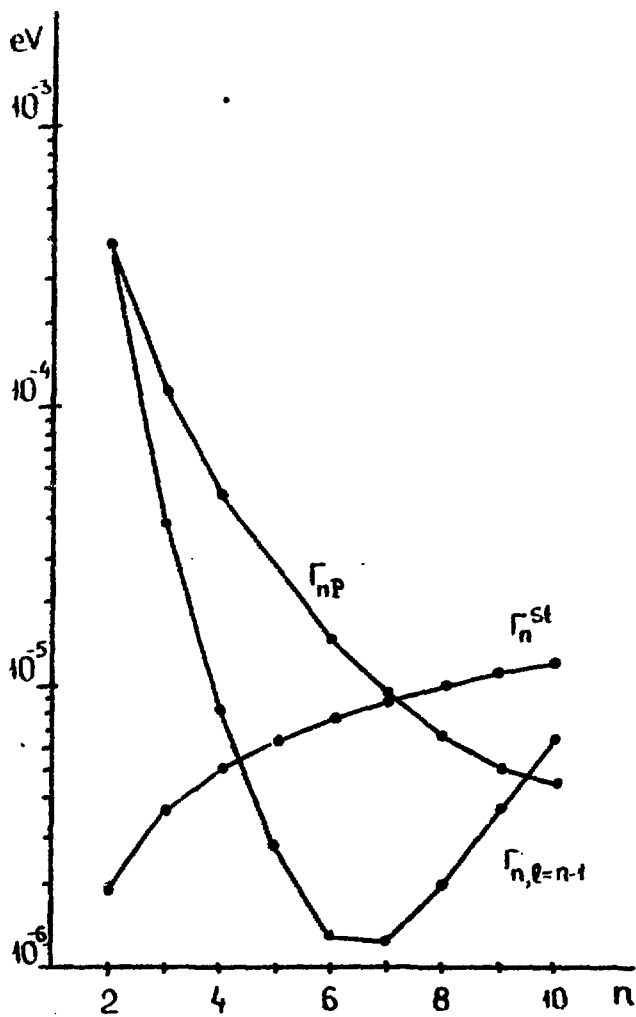


Fig. 6

The de-excitation (Γ_{nP} , $\Gamma_{n,\ell=n-1}$) and Stark mixing (Γ_n^{st}) rates in gaseous hydrogen ($N = 10^{-3}$ No., 0.8 atm, 300°K).

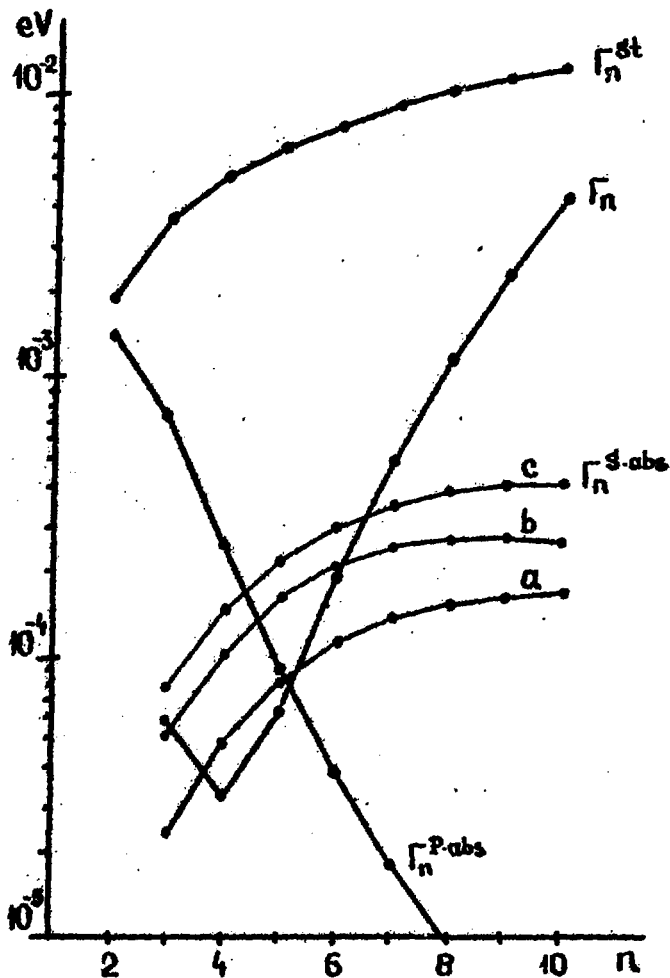


Fig. 7

The effective de-excitation and absorption rates in liquid hydrogen ($U = 10^6$ cm/sec):

- Γ_n - the total de-excitation rate,
- Γ_n^{P-abs} - the rate of the P state absorption for $\Gamma_{2p}^a = 10^{-2}$ eV,
- Γ_n^{S-abs} - the rates of the S state absorption for
 - a) $\Gamma_{1s} = 200$ eV, $\Delta E_{1s} = 1000$ eV,
 - b) $\Gamma_{1s} = 200$ eV, $\Delta E_{1s} = 500$ eV,
 - c) $\Gamma_{1s} = 500$ eV, $\Delta E_{1s} = 500$ eV.

place at $2 < n < 7$.

For the P- states the absorption widths Γ_{nP}^a prevail over de-excitation ones at $n < 6 \div 7$ (see Fig.4). The P- state mixing, in contrast to the S- state one, is not suppressed by the strong interaction effects, so that the effective P- state absorption rate Γ_n^{P-abs} rapidly increases with n decreasing (Fig.7). It exceeds the effective de-excitation rate at $n \leq 5$ and the S- state absorption rate at $n < 5 \div 6$. So we anticipate that at low n ($n \leq 4$) the absorption mainly occurs from the P- states ^{/2/}. The total fraction of the P- state absorption depends on probability of $\bar{p}p$ atom to reach the low-lying states, this probability being governed by the S- wave absorption at higher levels.

Gaseous hydrogen

In this case the rates of the Stark mixing and the Auger de-excitation are diminished by the factor (N/N_0) in comparison with the liquid hydrogen ($N/N_0 = 5 \cdot 10^{-3}$ corresponds to 4atm, 300°K) that leads the radiative de-excitation to become dominant at $n \leq 7 - 9$ for $N/N_0 = 10^{-3} - 5 \cdot 10^{-3}$ (see Fig.5,6). The main point to be emphasized is that the Stark mixing rate does not exceed the de-excitation ones at lowlying levels $n \leq n_c$ ($n_c = 4$ for $N = 5 \cdot 10^{-3} N_0$, $n_c = 5-7$ for $N = 10^{-3} N_0$). Therefore the occupation probabilities of the n^l sublevels do not satisfy the statistical distribution for all the levels. However the statistical distribution is maintained at high n ($n > 5$ for $N = 5 \cdot 10^{-3} N_0$ and $n > 9$ for $N = 10^{-3} N_0$), so we can start the cascade calculations at $n = 10$ assuming the statistical distribution in l .

At the initial stage of the cascade where the de-excitation is mainly due to the nonradiative effects, the rates of which are proportional to the target density, the S state absorption via the Stark mixing at $n > n_c$ plays the same role as it does in liquid hydrogen. As soon as the $\bar{p}p$ atom has cascaded to the levels where the radiative de-excitation is the most important one, the S-state absorption becomes weak since the radiative de-excitation rates turn out to dominate those of the Stark mixing $n\ell \rightarrow nS$.

The P-state absorption via the Stark mixing is important only at levels $n \leq n_c$ where the rate of the Stark collisions Γ_n^{st} is not small in comparison with the de-excitation rates. If the P-state annihilation width Γ_{nP}^a is greater than Γ_n^{st} , it is the case for $N < 10^{-2} N_0$ and $n < 10$, then the effective rate of the P-state absorption approaches its upper limit

$$\Gamma_n^{P-abs} = \frac{3}{n^2} \Gamma_n^{st} \left(1 - \exp\left(-\frac{\Gamma_{nP}^{tot}}{\Gamma_n^{st}}\right) \right) \approx \frac{3}{n^2} \Gamma_n^{st}$$

The statistical weight factor $3/n^2$ suppressing the probability of the Stark transitions into the P states at high n , the P state absorption can compete with de-excitation only for $n \leq 8$ (see Fig. 5, 6). As a result we conclude that the P state absorption via the Stark mixing is significant at $3 < n \leq 8$ for $N = 5 \cdot 10^{-3} N_0$ and at $6 \leq n \leq 8$ for $N = 10^{-3} N_0$.

Detailed calculation of $\bar{p}p$ atomic cascade

The lack of firmly established experimental data on $\bar{p}p$ atom does not enable us to calculate the picture of cascade processes uniquely. However, we have managed to choose the example of the cascade which seems to be

in agreement with the bulk of the data available and allows to illustrate the main properties of $\bar{p}p$ atom.

We shall consider orthoprotonium, to which we ascribe the following nuclear widths and shift:

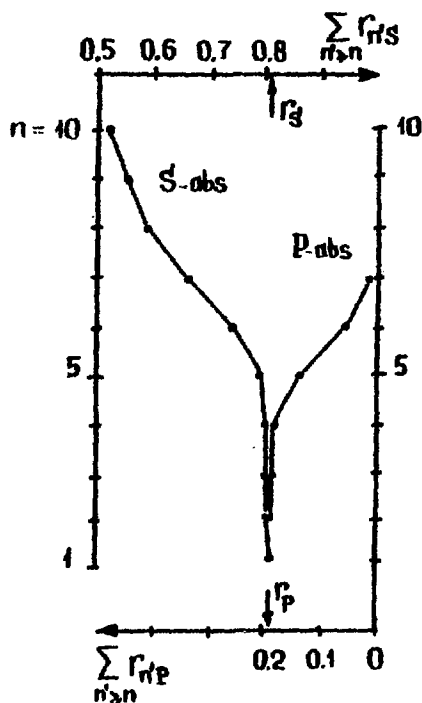
$$\begin{aligned} \Gamma_{1S} &= 200 \text{ eV} \\ \Delta E_{1S} &= 1 \text{ keV} \\ \Gamma_{2P}^a &= 10^{-2} \text{ eV} \end{aligned} \quad (31)$$

This magnitudes should not be taken too literally since there not any rigorous procedure to make the best fit of experimental data. The choice was based on the data in favour of the intensive P- wave absorption and on the results of measurement of gamma transitions between the levels of protonium and baryonium. The former concern the measurements the protonium X- rays in the gaseous target^{/11/} and the reaction $\bar{p}p \rightarrow 2\pi$ "at rest" ^{/9,10/}, which imply $\Gamma_{2P}^a \gtrsim 4 \cdot 10^{-3} \text{ eV}$ (the large value R_{S1} corresponds to this estimate, see ^{/2,3,20/}). Besides, the large shift of 1S level ($|\Delta E_{1S}| \sim 1 \text{ keV}$) is necessary to provide the large P wave contribution to the total absorption ^{/2,3,20/}. Gamma transitions intensities have already been considered in connection with the total 1S level width (Sec.4).

The level populations ρ_n , S and P wave absorption probabilities Γ_{nS} and Γ_{nP} and intensities of X ray transitions between atomic levels have been calculated for liquid and gaseous hydrogen ($N = 10^{-2} N_0$, $5 \cdot 10^{-3} N_0$, $10^{-3} N_0$) with the method described in Sec.3. The calculation was started from the level $n = 10$. The details of cascade at $n > 10$ are not of interest, mention only that according to the theoretical estimates^{/2,3/}

for given Γ_{1S} and ΔE_{1S} (30) about a half of initially formed $\bar{p}p$ atoms come down to the level $n = 10$, the rest of them being absorbed from S states, hence we have assumed $P_{10} = 0.5$. The $\bar{p}p$ atom velocity $U = 10^6$ cm/s corresponds to the kinetic energy 1 keV.

The level populations and absorption probabilities are shown in Fig. 8 and 9. In liquid hydrogen about 1/3 of all



n	P_n	r_{nS}	r_{nP}
10	0.500	0.020	0.0004
9	.463	.026	.0010
8	.437	.044	.0031
7	.394	.068	.011
6	.318	.085	.038
5	.197	.053	.084
4	.060	.0073	.047
3	.0064	.0005	.0055
2	.0023	.0007	.0025
1	.0050	.0050	-

$r_g = .81$ $r_p = .19$

Fig. 8

Capture schedule for protonium in liquid hydrogen ($\Gamma_{1S} = 200$ eV, $\Delta E_{1S} = 1$ keV, $\Gamma_{2P}^a = 10^{-2}$ eV, $\sigma = 10^6$ cm/sec): P_n are the total occupation probabilities, r_{nS} and r_{nP} - the S- and P- state absorption probabilities. The initial population is $P_{10} = 0.5$, with the previous absorption taking place in the S states ($r_g (n > 10) = 0.5$).

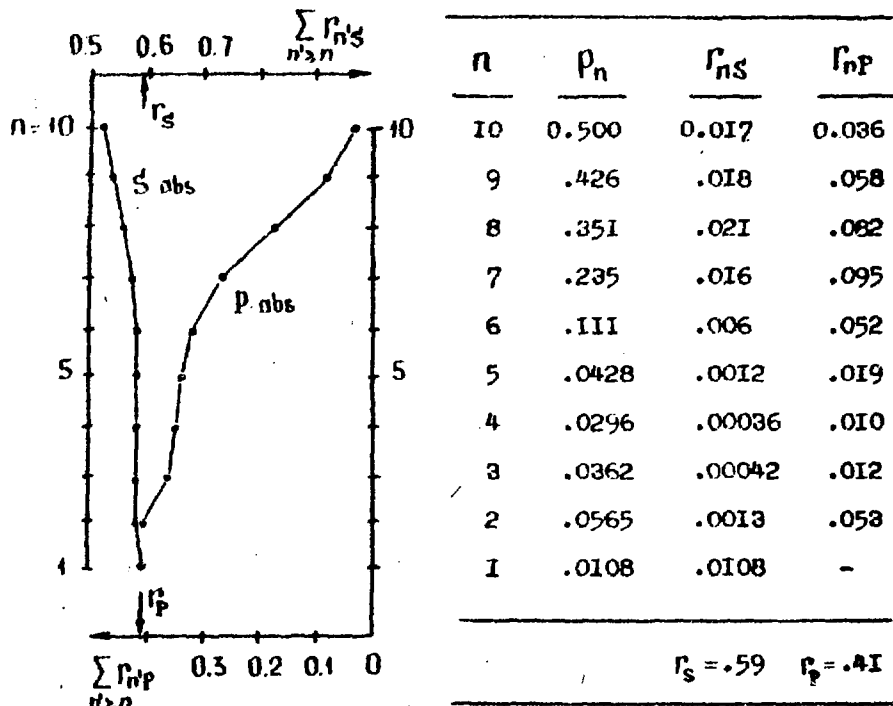


Fig. 9

Capture schedule for protonium in gaseous hydrogen
 ($N = 5 \cdot 10^{-3} N_0$, 4 atm, 300°K, $\Gamma_{1S} = 200$ eV,
 $\Delta E_{1S} = 1$ KeV, $\Gamma_{2P}^a = 10^{-2}$ eV, $v = 10^6$ cm/sec).

$\bar{p}p$ atoms reach the states with $n \leq 6$ where the P wave absorption becomes essential. The absorption by Stark mixing at levels $n = 4 \div 6$ proceeds so intensively that states with $n \leq 3$ are populated with very small probability $\rho_n < 10^{-2}$. The total P wave contribution to the absorption is $\rho_P = 0.19$.

In the gaseous hydrogen ($N = 5 \cdot 10^{-3} N_0$) the absorption by Stark mixing occurs only at high levels $n > 5$, the P wave absorption for $n = 6 \div 10$ being more

intensive than the S wave one. The total P wave absorption probability is $\Gamma_p = 0,41$.

The intensities of X ray transitions are given in Table 4 - 6, K and L lines intensities are also shown in Fig. 10 and 11.

Table 4

The X- rays yield of protonium in liquid hydrogen

$$\begin{aligned} \Gamma_{1s} &= 200 \text{ eV} \\ \Delta E_{1s} &= 1 \text{ KeV} \\ \Gamma_{2p}^a &= 10^{-2} \text{ eV} \end{aligned}$$

$Y_{n_i \rightarrow n_f}$ in units 10^{-3}

$n_i \backslash n_f$	1	2	3	4	5
8	0.08	0.04	0.03	0.03	0.03
7	0.27	0.16	0.12	0.11	0.12
6	0.95	0.57	0.46	0.46	0.63
5	2.12	1.36	1.20	1.51	-
4	1.24	0.93	1.04	-	
3	0.16	0.19	-		
2	0.10	-			
$\sum_{n_i} Y_{i \rightarrow f}$	4.95	3.28	2.88	2.13	0.79
P_{n_f}	4.95	3.33	6.40	60.0	197
$(\sum_{n_i} Y_{i \rightarrow f}) / P_{n_f}$	1.0	0.98	0.45	0.035	0.004

Table 5

The X - rays yield of protonium in gaseous hydrogen

(4 atm - $N = 5 \cdot 10^{-3} N_0$)

$$\Gamma_{1s} = 200 \text{ eV}$$

$$\Delta E_{1s} = 1 \text{ KeV}$$

$$\Gamma_{2p}^a = 10^{-2} \text{ eV}$$

$Y_{n_i \rightarrow n_f}$ in units 10^{-3}

$n_i \backslash n_f$	1	2	3	4	5	6
10	0.87	0.86	0.67	0.57	0.52	0.50
9	1.3	1.7	1.4	1.2	1.2	1.2
8	2.0	3.8	3.3	3.0	3.1	3.6
7	2.2	6.8	6.1	6.0	6.8	10.1
6	1.3	7.3	7.2	7.8	11.4	-
5	0.48	5.5	6.2	8.8	-	
4	0.27	7.4	11.1	-		
3	0.36	23.1	-			
2	2.02	-				
$\sum_{n_i} Y_{i \rightarrow f}$	10.8	56.5	36.0	27.6	23.1	15.5
P_{n_f}	10.8	56.5	36.2	29.6	42.8	111
$\frac{(\sum_{n_i} Y_{i \rightarrow f})}{P_{n_f}}$	1	1	0.996	0.93	0.54	0.14

Table 6

The X-rays yield of protonium in gaseous hydrogen

$$\Gamma_{1s} = 200 \text{ eV}$$

$$\Delta E_{1s} = 1 \text{ KeV}$$

$$\Gamma_{2p}^a = 10^{-2} \text{ eV}$$

$Y_{n_i \rightarrow n_f}$ in units 10^{-3}

n_i n_f	8 atm $N = 10^{-2} N_0$				0.8 atm $N = 10^{-3} N_0$			
	1	2	3	4	1	2	3	4
10	0.63	0.47	0.36	0.30	1.0	3.5	3.0	2.6
9	1.1	0.96	0.77	0.67	1.2	6.2	5.6	5.1
8	2.0	2.3	1.9	1.7	1.5	12	11	10
7	2.6	4.3	3.8	3.7	1.2	15	15	15
6	1.7	5.0	4.8	5.2	0.56	13	14	16
5	0.56	3.5	3.8	5.3	0.31	12	17	28
4	0.25	3.8	5.4	-	0.31	21	45	-
3	0.25	12	-	-	0.82	81	-	-
2	1.1	-	-	-	6.0	-	-	-
$\sum_{n_i} Y_{i \rightarrow f}$	10.2	32.0	20.8	16.8	12.8	164	110	77.5
P_{n_f}	10.2	32.0	21.0	19.4	12.8	164	111	78.5
$\frac{(\sum_{n_i} Y_{i \rightarrow f})}{P_{n_f}}$	1	1	0.99	0.87	1	1	0.998	0.985

In liquid hydrogen the radiative transitions provide 100% population of 1S level, 98% of 2P level population and 45% of $n = 3$ levels population, the higher levels being populated mainly by Auger transitions. The total K-lines intensity is $Y_K^{tot} = 5 \cdot 10^{-3}$, the main contribution coming from the initial states with $n = 4, 5, 6$ and only 2% from K_{α} line. The initial states with $n = 4, 5, 6$ dominate also in the L and M series. The reason is the populations of the low lying levels with $n < 4$ are small due to the absorption, while the radiative transitions at levels with $n > 6$ are suppressed by Auger effect.

In gaseous hydrogen ($N = 5 \cdot 10^{-3} N_0$) states with $n < 6$ are populated mainly by radiative transitions. The most intensive are L lines:

$$\begin{aligned} Y_{L\alpha} &= 2.3 \cdot 10^{-2} \\ Y_{L\beta} &= 0.74 \cdot 10^{-2} \\ Y_L^{tot} &= 5.6 \cdot 10^{-2} \end{aligned}$$

Lines of M series are rather intensive as well

$$\begin{aligned} Y_{M\alpha} &= 1.1 \cdot 10^{-2} \\ Y_M^{tot} &= 3.6 \cdot 10^{-2} \end{aligned}$$

Among K lines dominate the transitions from the states $n = 7, 8$. Intensities of K lines corresponding to the lower initial states are small due to the large annihilation widths of the nP states ($\Gamma_{nP}^a / \Gamma_{nP}^x \gg 1$) and due to the absence of the Stark mixing:

$$Y_{K\alpha} = 2 \cdot 10^{-3}$$

The difference between the protonium X rays spectra in liquid and gaseous hydrogen is displayed in Fig.10. The qualitative picture of the spectrum is kept the same when

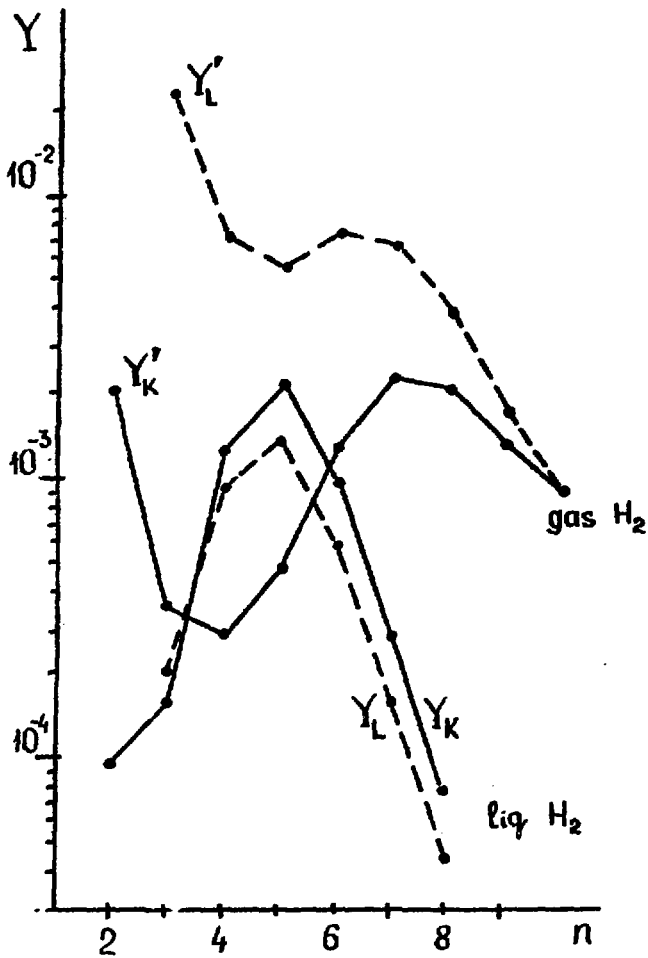


Fig.10 The yields of K and L lines of protonium in liquid and gaseous ($N = 5 \cdot 10^{-3} N_0$) hydrogen ($\Gamma_{1s} = 200$ eV, $\Delta E_{1s} = 1$ KeV, $\Gamma_{2p}^a = 10^{-2}$ eV, $P_{10} = 0.5$).

the quantities Γ_{1S} , ΔE_{1S} and Γ_{2P}^a are varied in rather wide interval, provided $|\Delta E_{1S}| \gtrsim 0.5 \text{ keV}$ and $\Gamma_{2P}^a \gg \Gamma_{2P}^x$. For an example we demonstrate in Fig.11 the intensities of K and L lines for the following set of nuclear parameters: $\Gamma_{1S} = 500 \text{ eV}$, $\Delta E_{1S} = 500 \text{ eV}$, $\Gamma_{2P} = 10^{-2} \text{ eV}$.

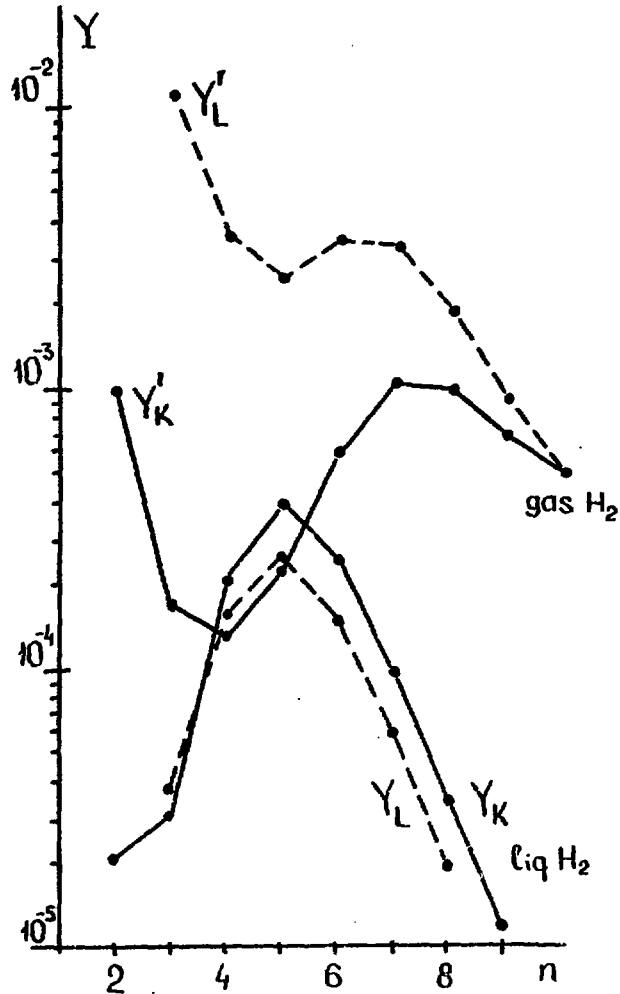


Fig.11 The yields of K and L lines of protonium in liquid and gaseous ($N = 5 \cdot 10^{-3} N_0$) hydrogen for the more intensive S-state absorption ($\Gamma_{1S} = 500 \text{ eV}$, $\Delta E_{1S} = 500 \text{ eV}$, $\Gamma_{2P}^a = 10^{-2} \text{ eV}$, $P_{10} = 0.33$).

6. COMPARISON OF THE THEORETICAL CALCULATIONS

WITH THE EXPERIMENTAL DATA

Our choice of nuclear parameters Γ_{1s} , ΔE_{1s} and Γ_{2p}^a provides good agreement of the cascade calculation with the following experimental data:

1. Reaction $\bar{p}p \rightarrow 2\pi$ at rest in liquid hydrogen

experiment

$$\Gamma_p = \begin{cases} 0.13 \pm 0.04 / 10 / \\ 0.39 \pm 0.08 / 9 / \end{cases}$$

theory

$$\Gamma_p = 0.19$$

2. X-ray yield of $\bar{p}p$ atom in gaseous hydrogen

experiment /11/

$$Y_{L\alpha} = 2 \cdot 10^{-2}$$

$$Y_{L\beta} = 1.7 \cdot 10^{-2}$$

$$Y_L^{tot} = 6 \cdot 10^{-2}$$

$$Y_{K\alpha} \leq 6 \cdot 10^{-3}$$

theory

$$Y_{L\alpha} = 2.3 \cdot 10^{-2}$$

$$Y_{L\beta} = 0.7 \cdot 10^{-2}$$

$$Y_L^{tot} = 5.6 \cdot 10^{-2}$$

$$Y_{K\alpha} = 2 \cdot 10^{-3}$$

3. γ -transitions between the levels of protonium and baryonium

experiment /5/

$$Y^i = (0.5 \pm 1) \cdot 10^{-2}$$

theory

$$Y^i = 0.6 \cdot 10^{-2}$$

$$K = 3/4$$

$$\Gamma_{1s}^{\gamma i} = 2 \text{ eV}$$

We conclude that the experimental data /5,9,10,11/ are self-consistent and the set of nuclear parameters Γ_{1s} , ΔE_{1s} and Γ_{2p}^a chosen above seems to be close to the true one for orthoprotonium. However the data on the relative intensities of X-rays K series of the protonium in liquid hydrogen /12/ appear to be in contradiction with our

theoretical results. The point is that the ratios of the intensities of experimentally observed lines (identified as K_{α} , K_{β} and K_{γ}):

$$Y_{K_{\alpha}} : Y_{K_{\beta}} : Y_{K_{\gamma}} = 2.3 : 2 : 1 \quad (32)$$

(the other lines are unseen) cannot be reproduced in calculations by any variation of nuclear parameters: the most intensive are the transitions from the initial states $n = 4 \div 6$ (both for ortho and paraprotonium). E.g., for the case considered above:

$$Y_{K_{\alpha}} : Y_{K_{\beta}} : Y_{K_{\gamma}} : Y_{K_{\delta}} = 1 : 1.5 : 12 : 24 \quad (33)$$

More than that, the cited above experimental relation does not seem to be self-consistent. To show this, consider the population of 2P level (only the radiative transitions to the 2P state are essential)

$$P_{2P} = \sum_{n \geq 3} Y_{nD \rightarrow 2P} \quad (34)$$

Taking into account that the Stark mixing between the states with $n > 3$ is more rapid than the de-excitation we obtain with the effective rates method the following relation:

$$\frac{Y_{nD \rightarrow 2P}}{Y_{nP \rightarrow 1S}} = \frac{5 \Gamma_{nD \rightarrow 2P}^X}{3 \Gamma_{nP \rightarrow 1S}^X} \quad (35)$$

Thus

$$P_{2P} = \sum_{n \geq 3} \frac{5 \Gamma_{nD \rightarrow 2P}^X}{3 \Gamma_{nP \rightarrow 1S}^X} Y_{nP \rightarrow 1S} \quad (36)$$

With the equality (Stark mixing $2P \rightarrow 2S$ unessential)

$$Y_{2P \rightarrow 1S} = \frac{\Gamma_{2P \rightarrow 1S}^X}{\Gamma_{2P}^{\text{tot}}} P_{2P} \quad (37)$$

we come to the final result

$$\frac{\Gamma_{2P}^{\text{tot}}}{\Gamma_{2P \rightarrow 1S}^X} = \sum_{n \geq 3} \frac{5 \Gamma_{nD \rightarrow 2P}^X}{3 \Gamma_{nP \rightarrow 1S}^X} \cdot \frac{Y_{nP \rightarrow 1S}}{Y_{2P \rightarrow 1S}} \quad (38)$$

Putting here the experimental values ^{/12/} we find

$$\frac{\Gamma_{2P}^{\text{tot}}}{\Gamma_{2P \rightarrow 1S}^X} = 0.8$$

while the ratio $\Gamma_{2P}^{\text{tot}}/\Gamma_{2P}^X$ should be more than unity (from the earlier experiments we expect that $\Gamma_{2P}^{\text{tot}}/\Gamma_{2P}^X \gg 1$). Thus, if the presented theoretical considerations are valid, then either the data on the relative intensities of X-ray transitions in ^{/12/} are incorrect, or the observed lines are not those of protonium K-series. But it is worth mentioning that the absolute yield of K_{α} - line by the order of the magnitude (10^{-4} per stopping antiproton) coincides with the theoretically expected one.

7. CONCLUSION

At present the theory of protonium is developed deeply enough to realize the phenomena of interest for the physics of nucleon-antinucleon interaction and their influence on the observed properties of $\bar{p}p$ atom. The experimental data available are, however, scarce and not rather reliable to allow somewhat unique and definite conclusions. The data on the intensities of γ transitions from protonium to baryonium states ^{/6/} are in agreement with the theoretical expectations. The independent data on the enhanced annihilation from protonium p-states (measurement of the process $\bar{p}p \rightarrow 2\alpha$ probability for the antiprotons stopping in liquid hydrogen ^{/9, 10/}) and on the X rays yield of protonium in gaseous target ^{/11/} do not contradict each other.

The yield of the X radiation ^{/12/} identified with protonium K lines agrees, by the order of magnitude, with the theory. But the data ^{/12/} on the relative intensities of the lines identified with K_{α} , K_{β} and K_{γ} can hardly be brought to agreement with the theoretical expectations.

The new generation of high precision experiments at LEAR (see ^{/30/}) will enable one to study protonium in vacuum in high precision experiments. However, the experiments with $\bar{p}p$ atoms in liquid and gaseous targets ^{/31-33/} still remain of interest. The theoretical methods developed above are also applicable to cascade processes in $\bar{p}d$ and $\bar{p}t$ atoms and to other light hadronic atoms ($K^{-}p$, $K^{-}d$, $\bar{\pi}^{-}p$, etc.).

The author is indebted to Dr. L.N.Bogdanova for many discussions about this work and Professor I.S.Shapiro for his advice.

References

1. I.S.Shapiro. Phys. Rep. 350, 131, 1978.
2. O.D.Dalkarov, B.O.Kerbikov, V.E.Markushin. Yad Fiz. 25, 853, 1977.
3. V.E.Markushin. Hadronic atoms. Lecture given at the 4th ITEP school on physics, in "Elementarnye chastitay" (Russ.) Vol.3, 58, Atomizdat, 1977.
4. O.D.Dalkarov, V.M.Samoilov, I.S.Shapiro. Sov. J. Nucl. Phys. 17, 566, 1973.
5. P.Pavlopoulos et al. Phys. Lett. 72B, 415, 1978.
6. A.E.Kudryavtsev, V.E.Markushin, I.S.Shapiro. Sov. JETP, 74, 225, 1978.
7. V.S.Popov, A.E.Kudryavtsev, V.D.Mur. ZhETF 77, 1727, 1979.
8. L.N.Bogdanova et al. Preprint ITEP-27, Moscow, 1975.
9. S.Devons et al. Phys. Rev. Lett. 27, 1614, 1971.
10. G.Bassompierre et al. Phys. Lett. 68B, 477, 1977.
11. E.G.Auld et al. Phys. Lett. 72B, 454, 1978.
12. M.Izycki et al. Paper contributed to the 4th European Antiproton Symp., Barr, France, 26-30 June 1978.
13. J.D.Davies et al. Phys. Lett. 83B, 55, 1979.
14. S.S.Gershtein et al. Preprint JINR, P4-12910, 1979.
15. T.B.Day, G.A.Snow, J.Sucher. Phys. Rev. Lett. 3, 61, 1959.
16. B.R.Desai. Phys. Rev 119, 1385, 1960.
17. M.Leon. H.A.Bethe. Phys. Rev. 127, 636, 1962.
18. M.Leon. Phys. Lett. 37B, 87, 1971.
19. V.E.Markushin. Preprint ITEP-164, Moscow, 1976.
20. B.O.Kerbikov, TH-2394-CERN, 1977.
21. A.S.Wightman. Phys. Rev. 77, 521, 1950.
22. P.K.Haff. T.A.Tombrello. Ann. of Phys. 86, 178, 1974.
23. S.Deser et al. Phys. Rev. 96, 774, 1954.

24. S.Gaser, R.Omnes. Phys. Lett. 39B, 369, 1972.
25. O.D.Dalkarov, V.M.Samoilov. JETP Lett 16, 249, 1972.
26. J.L.Vermaulen. Nucl. Phys. B12, 506, 1969.
27. J.Kemeni, J.Snell. Finit Markov chains. Moscow, 1970.
28. R.Bizzari et al. Nucl. Phys. B69, 307, 1974.
29. C.B.Dover. M.C.Zahse. Phys. Rev. Lett. 41, 438, 1978.
30. Proceedings of the Joint CERN-KfK-Workshop on Physics with Cooled Low Energetic Antiprotons, Karlsruhe, FRG, March 19-21, 1979.
31. Study of $\bar{p}p$ and $\bar{p}d$ Interaction at Threshold in Gaseous H_2 and D_2 Targets at LEAR, CERN-LAL-Mainz-München-TRIUMF-Zürich, CERN/PSCC/79-65/1 15, December 19, 1979.
32. Antiprotonic Atoms and Search for Baryonium at LEAR Basel-Karlsruhe-Stokholm-Strasbourg-Thessaloniki, CERN/PSCC/80-5/1 19, January 8, 1980.
33. Precision survey of K and L X-rays from $\bar{p}p$ ($\bar{p}d$) Atoms Birmingham Univ. - Rutherford Lab.-Surrey Univ. CERN/PSCC/80-9/1 20, January 14, 1980.



Маркушин В.Е.

Легкие экзотические атомы в жидком и газообразном водороде
и дейтерии. Атом $\bar{p}p$, теория и эксперимент

Работа поступила в ОНТИ 21/IV-1980г.

Подписано к печати 28/IV-80г. Т-07754. Формат 70x108 1/16.

Печ.л.3,0.Тираж 280 экз.Заказ 65.Цена 22 коп. Индекс 3624.

Отдел научно-технической информации ИТЭФ, ИИ7259, Москва

ИНДЕКС 3624